

29th International Cosmic Ray Conference Pune (2005) **00**, 101–106

HESS J1825-137: A pulsar wind nebula associated with PSR B1823-13?

O.C. de Jager^a, S. Funk^b, & J. Hinton^b for the H.E.S.S. Collaboration

(a) Unit for Space Physics, North-West University, Potchefstroom, South Africa

(b) Max-Planck-Institut für Kernphysik, Heidelberg, Germany

Presenter: O.C. de Jager (fskocdj@puk.ac.za), saf-dejager-OC-abs1.og22-oral

HESS J1825–137 was detected with a significance of 8.1σ in the Galactic Plane survey conducted with the H.E.S.S. instrument in 2004. Both HESS J1825–137 and the X-ray pulsar wind nebula G18.0–0.7 (associated with the Vela-like pulsar PSR B1823–13) are offset south of the pulsar, which may be the result of the SNR expanding into an inhomogeneous medium. The TeV size (~ 35 pc, for a distance of 4 kpc) is ~ 6 times larger than the X-ray size, which may be the result of propagation effects as a result of the longer lifetime of TeV emitting electrons, compared to the relatively short lifetime of keV synchrotron emitting electrons. The TeV photon spectral index of ~ 2.4 can also be related to the extended PWN X-ray synchrotron photon index of ~ 2.3 , if this spectrum is dominated by synchrotron cooling. The anomalously large size of the pulsar wind nebula can be explained if the pulsar was born with a relatively large initial spindown power and braking index $n \sim 2$, provided that the SNR expanded into the hot ISM with relatively low density ($\sim 0.003 \text{ cm}^{-3}$).

1. Introduction

PSR B1823–13 is a 101 ms evolved pulsar with a spin-down age of $T = 2.1 \times 10^4$ years (for an assumed braking index of $n = 3$) [4] and in these properties very similar to the Vela pulsar. It is located at a distance of $d = 3.9 \pm 0.4$ kpc [5]. High resolution *XMM-Newton* observations of the pulsar region confirmed a previous *ROSAT* detection of an asymmetric diffuse nebula, which was hence given the name G 18.0–0.7 [8]. For the compact core with extent $R_{\text{CN}} \sim 30''$ (CN: compact nebula) immediately surrounding the pulsar, a photon index of $\Gamma_{\text{CN}} = 1.6^{+0.1}_{-0.2}$ was measured with an unabsorbed luminosity of $L_{\text{CN}} \sim 9d_4^2 \times 10^{32} \text{ erg s}^{-1}$ in the 0.5 to 10 keV range for a distance of $4d_4$ kpc. The corresponding pulsar wind shock radius is $R_s \leq 15'' = 0.3d_4$ pc. The compact core is embedded in a region of extended diffuse emission which is clearly one-sided, revealing a structure south of the pulsar, with an extension of $R_{\text{EN}} \sim 5'$, (EN: extended nebula) whereas the $\sim 4'$ east-west extension is symmetric around the north-south axis. The spectrum of this extended component is softer with a photon index of $\Gamma_{\text{EN}} \sim 2.3$, with an unabsorbed luminosity of $L_{\text{EN}} = 3d_4^2 \times 10^{33} \text{ erg s}^{-1}$ for the 0.5 to 10 keV interval. No associated supernova remnant (SNR) has been identified yet.

2. A possible association of HESS J1825–137, G18.0–0.7 and 3EG J1826–1302

At γ -ray energies, PSR B1823–13 was proposed to power the close-by unidentified EGRET source 3EG J1826–1302 [6]. The region around PSR B1823–13 was observed as part of the survey of the Galactic plane with the H.E.S.S. instrument [1]. In this survey, a source of very high-energy (VHE) γ -rays (HESS J1825–137) $11'$ south of the pulsar was discovered with a significance of 8.1σ . We note, that the new VHE γ -ray source is located within the 95% positional confidence level of the EGRET source 3EG J1826–1302 and could therefore be related to this as of yet unidentified object. More details of the H.E.S.S. observations, analyses and merits of the possible association of HESS J1825–137 with G 18.0–0.7 was discussed by [2].

Figure 1 shows a north-south declination slice of G18.0–0.7 in X-rays and HESS J1825–137 in γ -rays. Both images show that the emission peaks at the position of PSR B1823–13, but with extended emission shifted

towards the south. The prominent X-ray synchrotron peak at the pulsar position is as a result of the compact X-ray nebula, where the magnetic field strength should be largest. Whereas the extent of the X-ray emission is only ~ 5 arcmin, the TeV emission is seen out to $\sim 0.5^\circ$. Even though the position of the unpulsed EGRET source 3EG J1826–1302 is consistent with that of HESS J1825–137 [2], the poor angular resolution of the EGRET instrument precludes a similar morphological study.

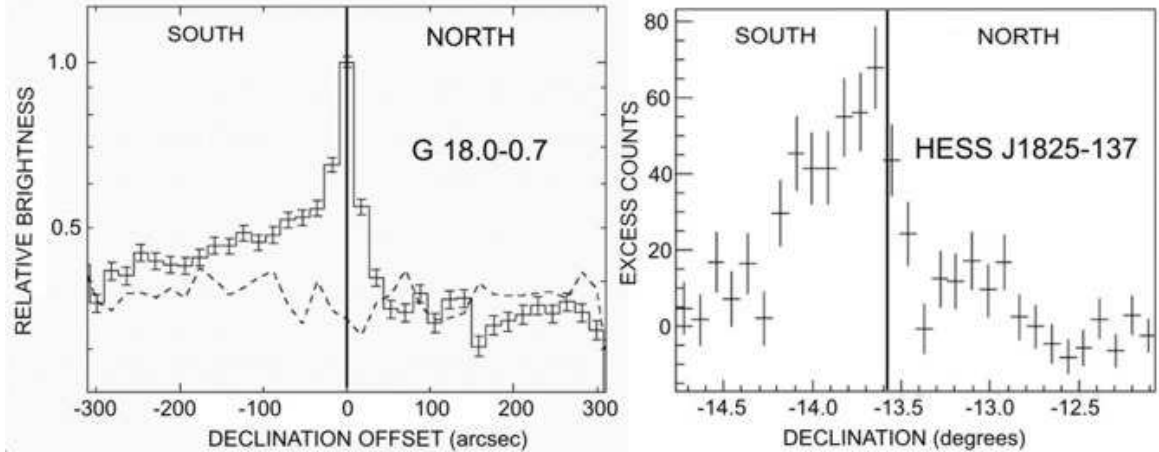


Figure 1. (a) left: north-south declination slice of G 18.0–0.7 in X-rays [8] showing the bright compact nebular core at the pulsar position and the $\sim 5'$ extended X-ray nebula extending to the south of PSR B1823–13 (indicated by a vertical line). (b) right: similar slice for HESS J1825–137, showing a similar extension south of the pulsar, but with a much larger size of $\sim 0.5^\circ$.

3. The one sided nature of the PWN and the anomalous size of HESS J1825–137

The one-sided nature of this PWN as seen in TeV was already suggested by [8], for the X-rays, based on the hydrodynamical simulations of [3] for Vela X and earlier studies referenced by [8]: It was assumed that the density of the interstellar medium (ISM) around the progenitor star was inhomogeneous along the north-south direction, with the density/pressure towards the northern direction significantly larger relative to the south. The reverse shock from the northern direction should then have crashed relatively early into the PWN, pushing the latter towards the south, as observed.

The remaining problem with the association of HESS J1825–137 with G18.0–0.7/PSR B1823–13 is the anomalously large size of the TeV source: the 0.5° diameter of the source translates to a radius of $R_{\text{PWN}} \sim 17d_4$ pc, and in the absence of radiative cooling in a SNR shell, one would expect a SNR forward shock radius of $R_{\text{SNR}} \sim 4R_{\text{PWN}} = 70d_4$ pc [9]. One possible key towards solving this problem would be to consider a relatively large initial spindown power (L_0) and pulsar braking index less than the canonical value of $n = 3$, which would increase the age T of the SNR. Integrating the spindown power $E_{\text{PSR}} = \int dt I\Omega\dot{\Omega}$ over the increased age would also maximise the PdV work done by the PWN against the SNR. The Sedov-Taylor SNR size would also increase with increasing age (scaling as $T^{2/5}$), giving a radius of

$$R_{\text{SNR}} = 78 \text{ pc} \left(\frac{E_{\text{SN}}}{10^{51} \text{ ergs}} \frac{0.003 \text{ cm}^{-3}}{N} \right)^{0.2} \left(\frac{1}{n-1} \right)^{0.4}.$$

Here $E_{SN} \sim 10^{51}$ ergs is the SN explosion energy and $N \sim 0.003 \text{ cm}^{-3}$ is the density of the hot phase of the ISM [7]. A pulsar braking index of $n = 2$ (“LMC pulsar” type) will increase the age of PSR B1823–13 to ~ 42 kyr if we assume a relatively large L_0 (i.e. an initial spin period much less than 0.1 s). This will imply a size consistent with the predicted size of ~ 70 pc.

Figure 2(a) shows the evolution of E_{PSR} with time for different values of n and L_0 : it is also clear that the total PWN energy is maximised for minimum n and maximal value of L_0 , but it is not yet clear how to relate this time dependent spindown power to the evolution of the PWN in a quantitave way.

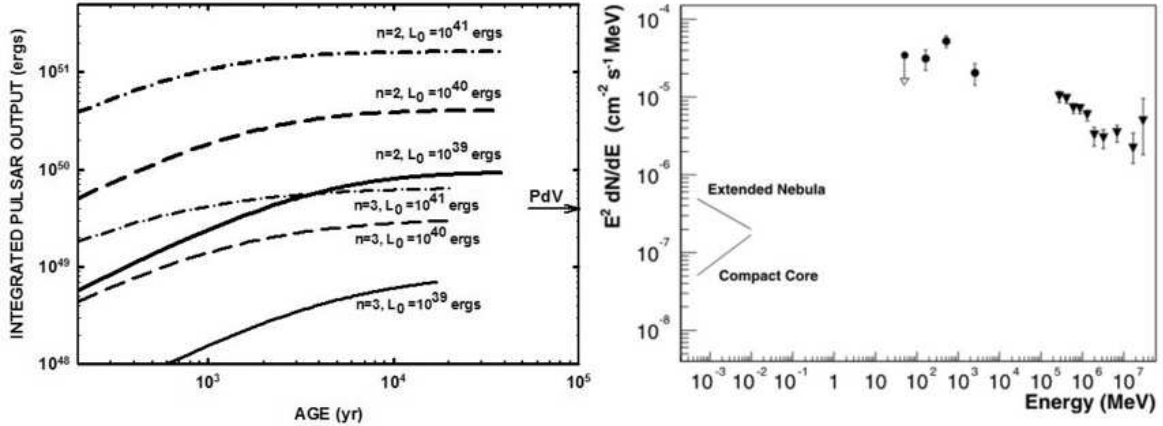


Figure 2. (a) left: integrated spindown power for PSR B1823–13 assuming different braking indices n and initial spindown power L_0 values as indicated. The arrow indicates the PdV work required to displace the observed PWN volume against a pressure of 5 eV/cm^3 . The vertical position of the arrow would then scale linearly with pressure. (b) right: the spectral energy distribution of the PWN of PSR B1823–13: HESS J1825–137 (triangles), G 18.0–0.7 (compact and extended nebula indicated by two lines) and 3EG J1826–1302 (circles). For details see [2].

4. The spectral energy distribution of the PWN of PSR B1823–13

Aharonian et al. [2] derived the spectrum of HESS J1825–137, which can be represented by a power law in energy, with photon index $2.40 \pm 0.09_{\text{stat}} \pm 0.2_{\text{sys}}$ and a flux above 230 GeV of $(3.4 \pm 0.2_{\text{stat}} \pm 0.8_{\text{sys}}) \times 10^{-11} \text{ cm}^{-2}\text{s}^{-1}$ (corresponding to 12% of the Crab flux above that energy). This spectrum is shown in Figure 2 (b), together with the X-ray spectra of G18.0–0.7 [8] and 3EG J1826–1302 [2]. It is clear that the TeV spectrum of HESS J1825–137 does not extrapolate towards GeV energies, and a spectral flattening below ~ 10 GeV is required. This spectral break may be the result of a cooling effect, which is also seen in X-rays: The compact nebular X-ray photon spectral index of ~ 1.6 represents the uncooled component, whereas the photon index of ~ 2.3 measured from the extended X-ray nebula, represents the synchrotron cooled component (as a result of propagation effects). The TeV photon index of ~ 2.4 is then consistent with inverse Compton scattering of these synchrotron cooled electrons on the CMBR, provided that this cooled spectrum also extends into the EUV/soft X-ray band, where electrons contribute directly to the observed TeV emission for a field strength of $\sim 10 \mu\text{G}$ or less.

The expected intrinsic break in the injected spectrum, represented by the so-called “ Γ -factor” of the wind at the pulsar wind shock of the compact nebula may also contribute to the observed flattening: in this case the number

spectrum of electrons with energy $E_e > \Gamma m_e c^2$ is expected to follow an accelerated power law spectrum of the form $E_e^{-2.2}$, resulting in the observed (uncooled) compact nebular spectrum with a photon index of 1.6 (as discussed above). Electrons with energy $E_e < \Gamma m_e c^2$ is then expected to have a much harder spectrum. This component is however unconstrained by radio or optical observations.

We also note that the energy flux in TeV is larger than the synchrotron energy flux of the extended X-ray nebula. This dominance of the TeV flux holds even if we extrapolate the spectrum of the extended X-ray nebula to the EUV/soft X-ray band. The evaluation of this soft synchrotron component is important, since electrons contributing to this soft unseen component, also scatter CMBR photons into the H.E.S.S. band for field strengths of $\sim 10\mu\text{G}$ or less: Note that the *XMM* X-ray spectrum is only measured within 5' from the pulsar, whereas electrons contributing to this soft band should have a much longer lifetime. They can therefore propagate to larger distances (as seen in TeV), resulting in a population of accumulated electrons over the lifetime of the pulsar, whereas the X-rays seen in Figure 2 (b) represent synchrotron emission from freshly injected electrons. This accumulation effect should increase the intensity of the soft component accordingly. Thus, the soft unseen synchrotron component should have a similar size as seen in TeV. A test for this hypothesis would be to measure the size of G 18.0–0.7 in the softest channels of *XMM* over an area similar to the TeV size. A more detailed study is however required to model the intensity of this unseen soft synchrotron component.

5. Appendix: lifetimes for X-ray and TeV emitting electrons

The respective synchrotron lifetimes of electrons in a transverse magnetic field of strength $B = 10^{-5}B_{-5}$ G, radiating synchrotron photons with mean energy E_{keV} (in units of keV) and inverse Compton scattered CMBR photons to a mean γ -ray energy of E_{TeV} (in units of TeV), are given by

$$\tau_X = 1.2 \text{ kyr} B_{-5}^{-3/2} E_{\text{keV}}^{-1/2} \quad \text{and} \quad \tau_\gamma = 4.8 \text{ kyr} B_{-5}^{-2} E_{\text{TeV}}^{-1/2}.$$

6. Acknowledgements

We thank Felix Aharonian, Luke Drury & Yves Gallant for useful discussions.

References

- [1] Aharonian, F.A. et al., (*H.E.S.S. Collaboration*) 2005a, *Science*, 307, 1938
- [2] Aharonian, F.A. et al., (*H.E.S.S. Collaboration*) 2005b, in preparation
- [3] Blondin, J.M., Chevalier, R.A., & Frierson, D.M. 2001, *ApJ*, 563, 806
- [4] Clifton, T. R., Lyne, A. G., Jones, A. W., McKenna, J., & Ashworth, M. 1992, *MNRAS*, 254, 177
- [5] Cordes, J. M., & Lazio, T. J. W. 2002, preprint (astro-ph/0207156)
- [6] Nolan, P. L., Tompkins, W. F., Grenier, I. A., & Michelson, P. F. 2003, *ApJ*, 597, 615
- [7] Ferriere, K. 1998, *ApJ*, 503, 700
- [8] Gaensler, B. M., Schulz, N. S., Kaspi, V. M., Pivovaroff, M. J., & Becker, W. E. 2003, *ApJ*, 588, 441
- [9] van der Swaluw, E., Achterberg, A., Gallant, Y. A., & Toth, G. 2001, *A&A*, 380, 309